Available online at www.sciencedirect.com
SCIENCE DIRECT®
Journal of Chromatography A, 1073 (2005) 63–73
JOURNAL OF CHROMATOGRAPHY A
www.elsevier.com/locate/chroma

Thermodynamic and kinetic characterization of nitrogen-containing polycyclic aromatic hydrocarbons in reversed-phase liquid chromatography

Victoria L. McGuffin*, Samuel B. Howerton, Xiaoping Li

Department of Chemistry, Michigan State University, East Lansing, MI 48824-1322, USA

Abstract

A series of five nitrogen-containing polycyclic aromatic hydrocarbons (NPAHs) was studied on polymeric octadecylsilica using methanol and acetonitrile as the mobile phase. The thermodynamic and kinetic behavior was examined as a function of ring number, annelation structure, and position of the nitrogen atom. The retention factors for the NPAHs are smaller than those for the parent PAHs in methanol, while the converse is true in acetonitrile. The changes in molar enthalpy are relatively comparable in both mobile phases with 1-aminopyrene having values of -5.0 ± 0.2 kcal/mol in methanol and -6.3 ± 0.7 kcal/mol in acetonitrile (1 cal = 4.184 J). However, the rate constants from mobile to stationary phase (k_{sm}) and from stationary to mobile phase (k_{ms}) demonstrate large differences as a function of mobile phase. For example, the rate constants k_{ms} for 1-aminopyrene and 4-azapyrene are 675 and 62 s^{-1}, respectively, in methanol at 303 K. In contrast, the same solutes demonstrate rate constants of 3.47 and 3.9×10^{-3} s^{-1}, respectively, in acetonitrile. The activation energies for transfer from mobile phase to transition state ($\Delta E_{\ddagger m}$) and from stationary phase to transition state ($\Delta E_{\ddagger s}$) also differ as a function of mobile phase. For example, the activation energies $\Delta E_{\ddagger s}$ for 1-aminopyrene are 21 and ~0 kcal/mol, whereas those for 4-azapyrene are 19 and 23 kcal/mol, in methanol and acetonitrile, respectively. Based on these thermodynamic and kinetic results, the relative contributions from the partition and adsorption mechanisms are discussed.

Keywords: Thermodynamics; Kinetics; Reversed-phase liquid chromatography; Polycyclic aromatic compounds; Azaarenes

1. Introduction

Polycyclic aromatic hydrocarbons (PAHs) are a class of compounds that present a recognized health hazard. As a result, many studies have been conducted to investigate the biological and chemical properties of these substances [1–3]. When formed at elevated temperatures, PAHs may contain substituent moieties that alter their toxicity. Two substitutions that lead to highly toxic analogues involve the exchange of a carbon atom with nitrogen to form an azaarene, and the replacement of a hydrogen atom with an amino or nitro group. These solutes are collectively known as nitrogen-containing polycyclic aromatic hydrocarbons (NPAHs). NPAHs are commonly found in fossil fuels and their derivatives, although some may also form during combustion processes.

Relative to their parent PAHs, NPAHs are more soluble in aqueous environments. Increased water solubility results in an increased potential for harm. For example, 1-aminopyrene demonstrates a 50-fold increase in mutagenic activity when compared to the parent PAH, pyrene [4]. Similarly, azaarenes demonstrate increased carcinogenicity when compared to their parent PAHs [5–7].

Studies have been carried out to determine the presence of NPAHs in fossil fuels [8–12], coal substitutes [13], lake sediment [14], urban aerosols [15], as well as from the degradation of polymers [16]. In order to identify and differentiate NPAHs, many investigators have used chromatographic techniques because of their high resolving power. These techniques have included gas [12,17,18], thin layer

* Corresponding author. Tel.: +1 517 355 9715; fax: +1 517 353 1793.
E-mail address: jgshabus@aol.com (V.L. McGuffin).

0021-9673/$ – see front matter © 2004 Elsevier B.V. All rights reserved.
doi:10.1016/j.chroma.2004.09.088

[19], supercritical fluid [20], and liquid chromatography [8–11,16,17,21–26]. In nearly all instances, the chromatographic applications have focused upon the optimization of the separation or upon qualitative and quantitative analysis, rather than a detailed examination of the molecular contributions to retention. The most noteworthy study by Colin et al. [21] examined the retention of 26 mono-substituted and 5 di-substituted aza-PAHs in reversed-phase liquid chromatography as a function of the mobile and stationary phase compositions. They reported that the aza-PAHs are separated on the basis of carbon number with aqueous methanol mobile phases and octadecylsilica stationary phases, whereas the position of the nitrogen atom(s) has a greater effect with aqueous tetrahydrofuran or acetonitrile mobile phases and octylsilica stationary phases. They observed dramatic tailing, which was attributed to interactions with unreacted silanol groups and/or the slow equilibrium between the neutral and protonated forms of the aza-PAHs. Although these observations suggest unusual thermodynamic and kinetic behavior, to the best of our knowledge, no quantitative explorations of this behavior have been published.

To overcome this dearth of information, the thermodynamics and kinetics of retention for a series of NPAHs are presented herein. Using theory and methodology developed previously for the characterization of PAHs [27,28], the retention factors and rate constants for the NPAHs are determined as a function of temperature and pressure. The effect of mobile phase is examined by using methanol as a model of protic solvents and acetonitrile as a model of aprotic solvents. From the retention factors, the changes in molar enthalpy and molar volume are quantitated. From the rate constants, the activation energy and activation volume are quantitated. This analysis provides insight into the retention mechanism of NPAHs in reversed-phase liquid chromatography.

2. Theory

As previously described [27,30], the calculation of thermodynamic and kinetic contributions to retention requires a synthesis of traditional thermodynamic and transition state theories. The thermodynamic parameters describe the path-independent measures of solute transfer from mobile to stationary phase. These parameters are calculated from the retention factor (k):

$$k = \frac{t_r - t_0}{t_0} \tag{1}$$

where t_r and t_0 are the elution times of a retained and non-retained solute, respectively. The retention factor is related to the changes in molar enthalpy (ΔH_{sm}) and molar entropy (ΔS_{sm}) by the Van't Hoff equation:

$$\ln k = \frac{-\Delta H_{sm}}{RT} + \frac{\Delta S_{sm}}{R} - \ln\beta \tag{2}$$

where R is the gas constant and T is the absolute temperature. The change in molar enthalpy is determined from the slope of a graph of the natural logarithm of the retention factor versus inverse temperature at constant pressure. The change in molar entropy is contained in the intercept, but cannot be reliably quantitated since the phase ratio (β) is a function of both temperature and pressure. From the definition of the molar enthalpy,

$$\ln k = \frac{-\Delta E_{sm} + T\,\Delta S_{sm} - P\,\Delta V_{sm}}{RT} - \ln\beta \tag{3}$$

which is a function of the molar internal energy (ΔE_{sm}) and the pressure–volume work ($P\,\Delta V_{sm}$). The change in molar volume (ΔV_{sm}) is determined from the slope of a graph of the natural logarithm of the retention factor versus pressure (P) at constant temperature.

The rate constant for transfer from stationary to mobile phase (k_{ms}) is given by:

$$k_{ms} = \frac{2kt_0}{\tau^2} \tag{4}$$

whereas the rate constant for transfer from mobile to stationary phase (k_{sm}) is given by:

$$k_{sm} = kk_{ms} = \frac{2k^2t_0}{\tau^2} \tag{5}$$

where τ represents the exponential contribution to variance that arises from slow mass transfer kinetics [27,30]. During this transfer, the solutes pass through a high-energy transition state (‡) that uniquely characterizes the path-dependent aspects of the retention mechanism. The kinetic rate constants can be expressed by means of the Arrhenius equation:

$$\ln k_{sm} = \ln A_{‡m} - \frac{\Delta E_{‡m}}{RT} \tag{6}$$

$$\ln k_{ms} = \ln A_{‡m} - \frac{\Delta E_{‡s}}{RT} \tag{7}$$

where $A_{‡m}$ and $A_{‡s}$ are the pre-exponential factors [27,30,31]. The activation energy ($\Delta E_{‡m}$ and $\Delta E_{‡s}$) is determined from the slope of a graph of the natural logarithm of the rate constant versus inverse temperature at constant pressure. From classical thermodynamic relationships [31,32],

$$\ln k_{sm} = \ln A_{‡m} - \frac{\Delta H_{‡m} + RT - P(\Delta V_{‡m})}{RT} \tag{8}$$

$$\ln k_{ms} = \ln A_{‡s} - \frac{\Delta H_{‡s} + RT - P(\Delta V_{‡s})}{RT} \tag{9}$$

The activation volume ($\Delta V_{‡m}$, $\Delta V_{‡s}$) is determined from the slope of a graph of the natural logarithm of the rate constant versus pressure at constant temperature. From the activation energy and activation volume, the activation enthalpy ($\Delta H_{‡m}$, $\Delta H_{‡s}$) can also be calculated. However, the activation enthalpy is influenced by the error in both the activation energy and activation volume and, thus, cannot always be reliably determined.

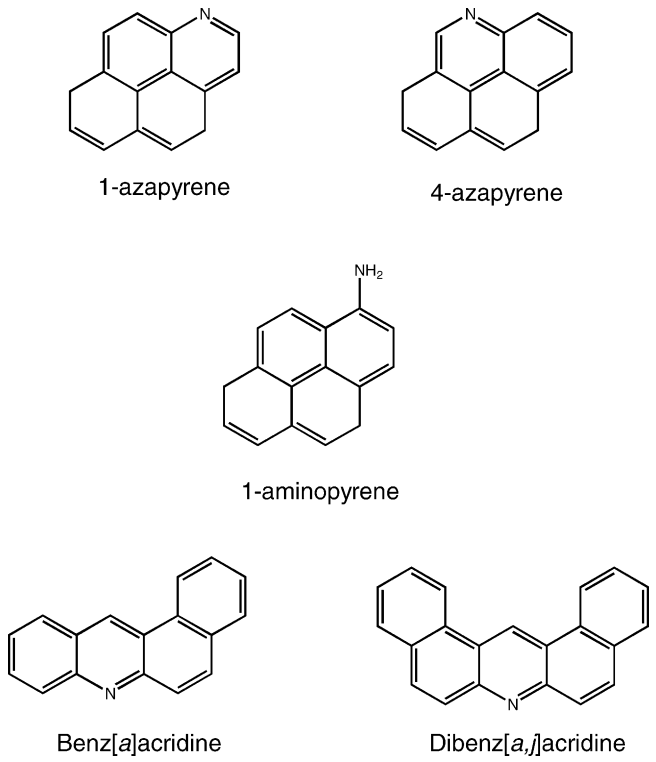

Fig. 1. Structure of the nitrogen-substituted polycyclic aromatic hydrocarbons (NPAHs).

3. Experimental

3.1. Chemicals

As depicted in Fig. 1, five NPAHs are chosen to study the effect of nitrogen position, ring number, and annelation structure on the thermodynamics and kinetics of retention. 1-Aminopyrene (Sigma–Aldrich), 1-azapyrene, 4-azapyrene, benz[*a*]acridine, and dibenz[*a,j*]acridine (Institüt für PAH Forschung) are obtained as solids and dissolved in high-purity methanol and acetonitrile (Burdick and Jackson, Baxter Healthcare) to yield standard solutions at a concentration of 10^{-4} M. A nonretained marker, 4-hydroxymethyl-7-methoxycoumarin [33], is added to each solution at a concentration of 10^{-4} M.

3.2. Experimental system

The solutes are separated on a capillary liquid chromatography system that has been described previously [27,33]. The column is a fused-silica capillary (76 cm × 200 μm i.d., Hewlett-Packard) that is packed via the slurry method and terminated with a quartz wool frit. Columns prepared by this method have very uniform packing across the diameter and along the length [34]. The silica packing is characterized by a 5.5 μm particle size, 190 Å pore size, and 240 m^2/g surface area (IMPAQ 200, PQ Corp.), reacted with trifunctional octadecylsilane to produce a polymeric phase with bonding density of 5.4 μmol/m^2. Although this stationary phase is not commercially available, it may be considered representative of high-density, polymeric octadecylsilica phases. The column has a plate height (H) of 15 μm, reduced plate height (h) of 2.73, total porosity (ε_T) of 0.84, and flow resistance parameter (ϕ) of 500. The column is operated at a nominal flow rate of 1.05 μL/min, linear velocity (v) of 0.055 cm/s, and reduced velocity (ν) of 2.75.

The methanol and acetonitrile mobile phases are delivered by a single-piston reciprocating pump (Model 114M, Beckman Instruments), operated in the constant-pressure mode. After injection (Model ECI4W1, Valco Instruments), the samples are split between the column and a fused-silica capillary (100 μm i.d., Polymicro Technologies), resulting in an injection volume of 10 nL. A fused-silica capillary (20 μm i.d., Polymicro Technologies) is attached to the column terminus to serve as a restrictor. By reducing the length of the splitter and restrictor proportionally, the pressure drop along the column is held constant as the average pressure is varied from 585 to 3585 psi (±15 psi) (1 psi = 6894.76 Pa). The column, injector, splitter, and restrictor are housed within a cryogenic oven (Model 3300, Varian Associates) that enables the temperature to be varied from 283 to 333 K (± 0.1 K).

The polyimide coating is removed from the capillary column at two positions (23.2 and 58.3 cm) to facilitate on-column detection by laser-induced fluorescence. The optical and electronic components of this system were designed and constructed in-house to ensure that all contributions to variance are identical at each detector position. A helium–cadmium laser (Model 3074-20 M, Melles Griot) provides excitation at 325 nm, which is transmitted to the column by a UV-grade optical fiber (100 μm, Polymicro Technologies). The fluorescence signal is collected orthogonal to the incident beam by a large diameter optical fiber (500 μm, Polymicro Technologies), isolated by a 420 nm interference filter (S10-410-F, Corion), and detected by a photomultiplier tube (Model R760, Hamamatsu). The resulting photocurrent is amplified, converted to the digital domain (Model PCI-MIO-16XE-50, National Instruments), and stored by a user-defined program (Labview v5.1, National Instruments).

3.3. Data analysis

After collection, the zone profile for each solute is extracted from the chromatogram using the previously established conditions for the minimum number of points, integration limits, and signal-to-noise ratio [35]. Each profile is fit by nonlinear regression to the exponentially modified Gaussian (EMG) and nonlinear chromatography (NLC) equations, which are discussed in the following sections, by using a commercially available program (Peakfit v4.14, SYSTAT Software). The resultant fitting parameters are then subtracted to determine the change between the two detectors. This method ensures that all measured changes in the solute zone profile

arise solely from processes occurring on the column. A result of using this method is that the upper limit for the rate constants can be expanded beyond that reported in previous work [27].

3.3.1. Exponentially modified Gaussian equation

The first model used to analyze the zone profiles is the exponentially modified Gaussian (EMG) equation. The EMG equation is chosen because the statistics of fit are better than for any other model that has been demonstrated to have physical meaning [30,35]. The EMG equation is the convolution of Gaussian and exponential functions, with the resulting form:

$$C(t) = \frac{A}{2\tau} \exp\left[\frac{\sigma^2}{2\tau^2} + \frac{t_g - t}{\tau}\right] \times \left[\operatorname{erf}\left(\frac{t - t_g}{\sqrt{2}\sigma} - \frac{\sigma}{\sqrt{2}\tau}\right) + 1\right] \quad (10)$$

where $C(t)$ is the concentration as a function of time, A is the peak area, t_g is the retention time of the Gaussian component, σ is the standard deviation of the Gaussian component, and τ is the exponential component. Symmetrical zone broadening, which arises from diffusion and mass transfer processes that are fast relative to the separation time, is quantified by σ. Asymmetrical broadening, which arises from volumetric sources (i.e., injectors, unions, etc.), electronic sources (i.e. amplifiers, etc.), and diffusion and mass transfer processes that are slow relative to the separation time, is quantified by τ. Because asymmetry from volumetric and electronic contributions is constant at each detector, the contribution from slow kinetics can be determined by difference between the two detectors. The resulting values of the EMG fitting parameters can be used to characterize the thermodynamic and kinetic behavior by means of Eqs. (1), (4), and (5), where

$$t_r = t_g + \tau \quad (11)$$

3.3.2. Nonlinear chromatography equation

The second model used to analyze the zone profiles is the nonlinear chromatography (NLC) equation. Initially described by Thomas [36], the current form of the NLC equation was developed by Wade et al. [37]

$$C(t) = \frac{a_0}{a_2 a_3}\left[1 - \exp\left(-\frac{a_3}{a_2}\right)\right] \times \left[\frac{\sqrt{(a_1/x)}I_1(2\sqrt{a_1 x/a_2})\exp((-x - a_1)/a_2)}{1 - T(a_1/a_2, x/a_2)\left[1 - \exp(-a_3/a_2)\right]}\right] \quad (12)$$

where

$$T(u, v) = e^{-v}\int_0^u e^{-t} I_0(\sqrt{2vt})\,dt \quad (13)$$

and I_0 and I_1 are modified Bessel functions of the first kind. The fitting parameters that are incorporated in the NLC model are the area (a_0), position (a_1), width (a_2), and distortion (a_3). If the chromatographic data are transformed from the time domain to the retention factor domain via Eq. (1), then these parameters can be used to calculate the lumped desorption rate constant:

$$a_2 = \frac{1}{k_{ms} t_0} \quad (14)$$

Using the established relationship between the retention factor and the rate constants ($k = k_{sm}/k_{ms}$), the adsorption rate constant can also be calculated.

4. Results and discussion

Based on previous experience with the parent PAHs [27,28], the EMG function was chosen for regression of the NPAH zone profiles in initial studies. The zone profiles in methanol mobile phase, shown in Fig. 2A, are similar to those observed in previous studies. The overall quality of fit is high, exhibiting random residuals and large values for the square of the correlation coefficient ($R^2 > 0.98$) and F-statistic ($F > 1000$). However, the zone profiles in acetonitrile mobile phase, shown in Fig. 2B, are quite different and demonstrate a much higher degree of asymmetry. This asymmetry may arise from a change in retention mechanism from partition to either adsorption or mixed mode partition–adsorption. As a result, the zone profiles in acetonitrile were analyzed by using the NLC model, which was thought to be more appropriate for the adsorption mechanism. However, the NLC model failed to produce any improvement in the quality of fit ($R^2 > 0.95$, $F > 1000$). Moreover, the zone profiles did not change as a function of concentration, which suggests that the isotherm is linear rather than nonlinear. Consequently, the EMG model was used throughout this study to provide consistency in the thermodynamic and kinetic results.

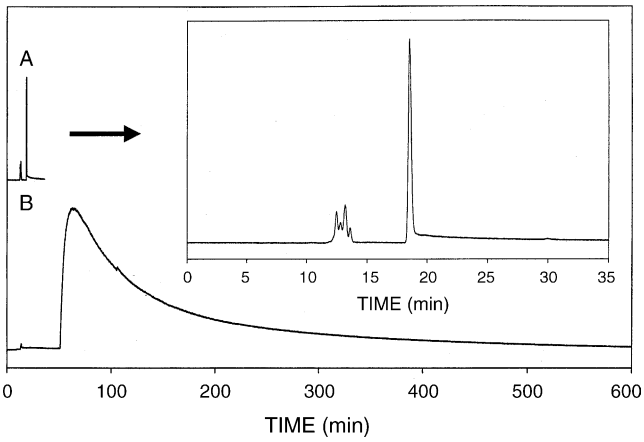

Fig. 2. Representative chromatograms of 4-azapyrene in reversed-phase liquid chromatography. Column: polymeric octadecylsilica. Mobile phase: (A) methanol, 303 K, 2085 psi, 0.08 cm/s; (B) acetonitrile, 303 K, 2185 psi, 0.08 cm/s. Column: polymeric octadecylsilica. Other experimental details as given in the text.

Table 1
Retention factors for NPAHs in methanol mobile phase

Solute	k[a]		k[b]	
	288 K	303 K	585 psi	3585psi
1-Aminopyrene	0.35	0.23	0.35	0.35
1-Azapyrene	0.94	0.52	0.95	0.94
4-Azapyrene	0.78	0.48	0.79	0.78
Benz[*a*]acridine	1.03	0.58	0.97	1.03
Dibenz[*a*,*j*]acridine	3.26	1.52	2.96	3.26

[a] Retention factor (k) calculated at $P = 3585$ psi.
[b] Retention factor calculated at $T = 288$ K.

4.1. Methanol mobile phase

4.1.1. Thermodynamic behavior

4.1.1.1. Retention factor. Representative values of the retention factor for the NPAHs in methanol mobile phase are summarized in Table 1. The retention factors for the NPAHs are notably smaller than those for the parent PAHs on the same stationary phase [27,28]. 1-Aminopyrene, 1-azapyrene, and 4-azapyrene have retention factors that are smaller by 73%, 38%, and 43%, respectively, than pyrene ($k = 0.84$ at 303 K). Similarly, the retention factor for benz[*a*]acridine is 60% smaller than that for benz[*a*]anthracene ($k = 1.46$ at 303 K). This decreased retention is due to the increased polarity of the NPAHs relative to the PAHs. Because the partition mechanism is governed by differences in relative solubility in the polar mobile phase and nonpolar stationary phase [38], the more polar NPAHs are less retained. It is noteworthy that the trends in retention factor for the NPAHs are the same as those identified previously for the PAHs. Retention increases with the number of aromatic rings [27] and decreases with more condensed annelation structure [28] or length-to-breadth ratio [29]. These trends are consistent with the partition mechanism.

As shown in Table 1, the retention factor for all solutes decreases significantly (34–53%) with increasing temperature. The retention factor increases slightly (6–10%) with increasing pressure for benz[*a*]acridine and dibenz[*a*,*j*]acridine, but remains statistically invariant for the amino- and azapyrenes. The reasons for this behavior are discussed below in further detail.

4.1.1.2. Molar enthalpy. A representative graph of the logarithm of the retention factor versus the inverse temperature (Van't Hoff plot) is shown in Fig. 3. The data for the methanol mobile phase are represented using solid lines. The graph for each solute is linear ($R^2 = 0.986$–0.999) and the slope is positive. A linear graph indicates that the change in molar enthalpy is constant, which suggests that there is no significant change in retention mechanism over the temperature range of 283–303 K. A positive slope is indicative of a negative change in molar enthalpy, which suggests that the transfer from mobile to stationary phase is enthalpically favorable. The change in molar enthalpy is calculated from the slope of Fig. 3, according to Eq. (2).

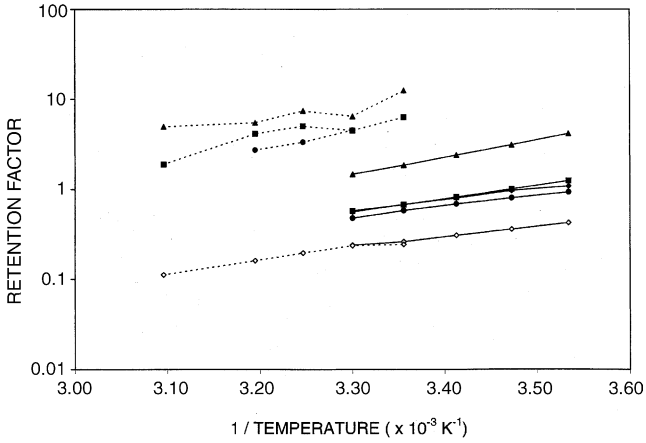

Fig. 3. Representative graph of the retention factor vs. inverse temperature used to calculate the change in molar enthalpy. Mobile phase: methanol, 2085 psi, 0.08 cm/s (—); acetonitrile, 2185 psi, 0.08 cm/s (– – –). Solutes: 1-aminopyrene (◊), 1-azapyrene (♦), 4-azapyrene (●), benz[*a*]acridine (■), dibenz[*a*,*j*]acridine (▲). Other experimental details as given in the text.

As shown in Table 2, the changes in molar enthalpy are the least negative for 1-aminopyrene, are comparable for 1-azapyrene and 4-azapyrene, and become progressively more negative for benz[*a*]acridine and dibenz[*a*,*j*]acridine. These changes in molar enthalpy follow the same trends as observed for the parent PAHs [27,28]. These trends indicate that the change in molar enthalpy becomes more negative with increasing ring number and with less condensed annelation structure. The reasons for these trends have been discussed previously [28] and may be attributed to the depth to which each PAH can penetrate into the stationary phase. The proximal regions, where the alkyl group is bound to the silica surface, are highly ordered with all trans carbon–carbon bonds. As the distance from the surface increases there are more gauche bonds and greater disorder [39,40]. The more condensed PAHs, such as pyrene, probe only the distal regions, whereas less condensed PAHs, such as benz[*a*]anthracene, can penetrate more deeply into the ordered regions of the stationary phase. Consequently, the change in molar enthalpy becomes more negative the farther the PAH penetrates into the stationary phase.

When compared to the parent PAH, pyrene ($\Delta H_{sm} = -4.4$ kcal/mol [28], 1 cal = 4.184 J), the change in molar enthalpy is 0.6 kcal/mol more negative for 1-

Table 2
Changes in molar enthalpy and molar volume for NPAHs in methanol mobile phase

Solute	ΔH_{sm} (kcal/mol)[a]	ΔV_{sm} (mL/mol)[b]
1-Aminopyrene[c]	-5.0 ± 0.2	-1.7 ± 2
1-Azapyrene	-5.7 ± 0.3	-0.1 ± 4
4-Azapyrene	-5.6 ± 0.2	-1.5 ± 5
Benz[*a*]acridine	-6.6 ± 0.1	-6.8 ± 1
Dibenz[*a*,*j*]acridine	-8.9 ± 0.1	-10.7 ± 1

[a] Molar enthalpy (ΔH_{sm}) calculated at $P = 2085$ psi.
[b] Molar volume (ΔV_{sm}) calculated at $T = 288$ K, except as otherwise noted.
[c] Molar volume calculated at $T = 283$ K.

aminopyrene and 1.2–1.3 kcal/mol more negative for the azapyrenes on the same stationary phase. Interactions with the octadecyl groups are relatively similar for these solutes. Hence, the differences may arise from interactions with silanol groups, either on the silica surface or on incompletely reacted and hydrolyzed molecules of the trifunctional octadecylsilane [21,41]. The PAHs interact very weakly with the silanol sites by hydrogen bonding through the aromatic (π) system. The nitrogen atom imparts a more basic character to the NPAHs, relative to the parent PAHs, that allows for stronger interaction with the acidic silanol sites [42,43]. This interaction is stronger than a simple hydrogen bond, but not as strong as proton transfer [43]. The amine group is less basic than the aza group, as evidenced by the acid–base equilibrium constants of aniline ($pK_a = 4.63$) and pyridine ($pK_a = 5.25$) [44]. Thus, the change in molar enthalpy for 1-aminopyrene is expected to be less than that for the azapyrenes, as observed in Table 2. The molar enthalpy for 4-azapyrene is less than that for 1-azapyrene because diffusion through the octadecyl groups to the silanol sites is more facile along the short axis than along the long axis of the molecule. It is also evident that the change in molar enthalpy for benz[*a*]acridine is 0.5 kcal/mol less negative than that for the parent PAH, benz[*a*]anthracene ($\Delta H_{sm} = -7.1$ kcal/mol [28]). Given the position of the nitrogen atom, diffusion must occur along the long axis of the molecule in order to bind with the silanol groups. This is much less favorable for the linear structure of benz[*a*]acridine than for the condensed structure of the azapyrenes. Similar steric effects are expected for dibenz[*a*,*j*]acridine, whose molar enthalpy is 6.9 kcal/mol less negative than the structurally similar five-ring PAH, picene [28].

Although there have been no published studies on the thermodynamics of retention for NPAHs in reversed-phase liquid chromatography, supporting evidence is provided from other separation techniques. Woodrow and Dorsey examined the partitioning of acridine in micellar electrokinetic chromatography [45]. They report an enthalpy of transition between the alkyl group of the surfactant and water as −6.75 kcal/mol for this solute. Matzner and Bales examined the retention of acridine on silica in aqueous media [46,47]. They report an enthalpy of transition between silica and water as –8.05 kcal/mol. These results support our suggestion that the more negative values of enthalpy for the four-ring NPAHs relative to their parent PAHs are due to interactions with the silica surface.

Finally, it is important to note that the retention factors for the NPAHs are smaller than those of the parent PAHs, even though the changes in molar enthalpy are more negative. There are two potential reasons for this phenomenon. First, there may be a significant entropic effect that offsets the enthalpic contributions to retention. For example, Matzner and Bales report values for the entropy term ($T\,\Delta S_{sm}$) as −5.09 kcal/mol compared with the enthalpy term of −8.05 kcal/mol for adsorption of acridine on silica [46,47]. Second, the phase ratio for the silanol sites may be very small relative to the octadecyl groups because of the high bonding density (5.4 μmol/m^2). According to Eq. (2), either a significant change in the entropy term or the phase ratio would allow the retention factors for the NPAHs to remain smaller than those of the parent PAHs, despite the greater changes in molar enthalpy. As both of these contributions are contained in the intercept of the Van't Hoff plot, they are difficult to distinguish by chromatographic methods alone.

4.1.1.3. Molar volume. A representative graph of the logarithm of the retention factor versus pressure is shown in Fig. 4. Although the graph for each NPAH is linear, the square of the correlation coefficient is highly variable ($R^2 = 0.594$–0.998) because of the small influence of pressure on retention. It should be noted that the smallest correlation coefficients are exhibited by the azapyrenes, which are affected the least by changes in pressure. The slope of the graph is positive for all solutes, which is indicative of a negative change in molar volume. This suggests that the solute occupies less volume in the stationary phase than in the mobile phase. The change in molar volume is calculated from the slope of this graph, according to Eq. (3).

As shown in Table 2, 1-aminopyrene, 1-azapyrene, and 4-azapyrene have values that are statistically indistinguishable and close to zero. In contrast, benz[*a*]acridine and dibenz[*a*,*j*]acridine exhibit changes in molar volume that are statistically nonzero, with the four-ring NPAH demonstrating a less negative change in molar volume than the five-ring analogue. The values for the azapyrenes and benz[*a*]acridine are similar to those for the parent PAHs, pyrene (−2.3 mL/mol) and benz[*a*]anthracene (−8.4 mL/mol) [28]. As noted previously, these changes in molar volume may be attributed to the depth that each PAH can penetrate into the stationary phase [27,28]. The more condensed PAHs, such as pyrene, probe only the distal regions, whereas less condensed PAHs, such as benz[*a*]anthracene, can penetrate more deeply into

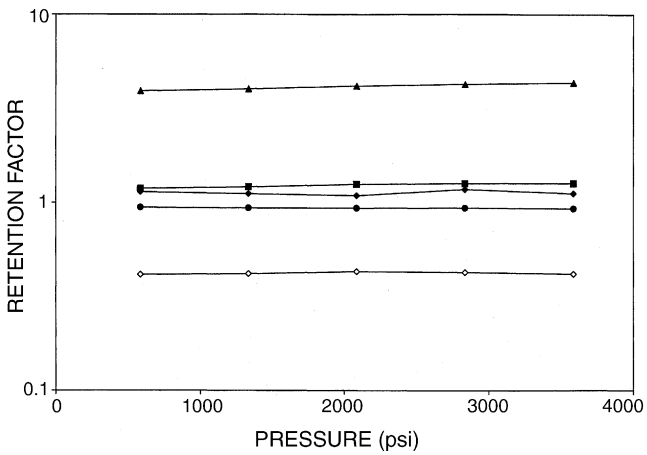

Fig. 4. Representative graph of the retention factor vs. pressure used to calculate the change in molar volume. Mobile phase: methanol, 283 K, 0.08 cm/s. Symbols defined in Fig. 3. Other experimental details as given in the text.

Table 3
Rate constants for NPAHs in methanol mobile phase

Solute	k_{ms} (s^{-1})[a]		k_{sm} (s^{-1})[a]		k_{ms} (s^{-1})[b]		k_{sm} (s^{-1})[b]	
	288 K	303 K	288 K	303 K	585 psi	3585 psi	585 psi	3585 psi
1-Aminopyrene	149	675	52	154	351	149	124	52
1-Azapyrene	0.7	4	0.7	2	0.8	0.7	0.7	0.7
4-Azapyrene	18	62	14	30	14	18	11	14
Benz[*a*]acridine	14	80	14	47	18	14	17	14
Dibenz[*a*,*j*]acridine	6	49	21	75	9	6	27	21

[a] Rate constants from stationary to mobile phase (k_{ms}) and from mobile to stationary phase (k_{sm}) calculated at $P = 3585$ psi.
[b] Rate constants calculated at $T = 288$ K.

the ordered regions of the stationary phase. Consequently, the change in molar volume becomes more negative the farther the PAH penetrates into the stationary phase.

4.1.2. Kinetic behavior

Although the thermodynamic data demonstrate the steady-state aspects of chromatographic behavior, they do not fully explain the retention mechanism. Using the equations and methods developed above, the pseudo-first-order rate constants, activation energies, and activation volumes were calculated. These values help to quantify the kinetic aspects of mass transfer between the mobile and stationary phases as a function of solute structure. These data provide information about the retention mechanism that would not be available from thermodynamic data alone.

4.1.2.1. Rate constants. Representative values of the rate constants, calculated using Eqs. (4) and (5), are summarized in Table 3. 1-Aminopyrene undergoes the fastest rate of transfer, followed by 4-azapyrene, benz[*a*]acridine, and dibenz[*a*,*j*]acridine. 1-Azapyrene has the slowest rate of transfer, with rate constants that are one order-of-magnitude less than 4-azapyrene and two orders-of-magnitude less than 1-aminopyrene. The rate-limiting step for 1-aminopyrene, 1-azapyrene, 4-azapyrene, and benz[*a*]acridine is the transfer from mobile to stationary phase, since the retention factor ($k = k_{sm}/k_{ms}$) is less than unity. In contrast, the rate-limiting step for dibenz[*a*,*j*]acridine is the transfer from stationary to mobile phase, since the retention factor is greater than unity.

The rate constants for the four-ring NPAHs are notably smaller than those for their parent PAHs on the same stationary phase [28]. 1-Aminopyrene, 1-azapyrene, and 4-azapyrene have rate constants that are smaller by 71%, 99.8%, and 97%, respectively, than pyrene ($k_{ms} = 2300\ s^{-1}$ at 303 K). Similarly, the rate constant for benz[*a*]acridine is 91% smaller than that for benz[*a*]anthracene ($k_{ms} = 850\ s^{-1}$ at 303 K). In contrast, the rate constant for the five-ring NPAH, dibenz[*a*,*j*]acridine, is more comparable to that for the five-ring PAH, picene [27]. These results suggest that 1-azapyrene is most greatly affected, 4-azapyrene and benz[*a*]acridine are moderately affected, and dibenz[*a*,*j*]acridine is relatively unaffected by the slow kinetics of adsorption at silanol sites.

As shown in Table 3, the rate constants for all solutes increase significantly (240–720% for k_{ms}) with increasing temperature. This behavior is a consequence of the increased diffusion coefficients and the enhanced fluidity of the stationary phase. As more kinetic energy is imparted, the alkyl chains become more labile and can more readily undergo rotation of the carbon–carbon bonds from the trans to gauche conformation. In fact, an order–disorder phase transition has been reported previously for this stationary phase at approximately 318 K [33]. The rate constants decrease significantly (58% for k_{ms}) with increasing pressure for 1-aminopyrene, but decrease only slightly or remain invariant for the other solutes. This behavior is a consequence of the compression of the alkyl chains, which impedes diffusion into and out of the stationary phase.

4.1.2.2. Activation energy. A representative graph of the logarithm of the rate constant versus the inverse temperature is shown in Fig. 5. The data for the methanol mobile phase are represented using solid lines. The graph for each solute is linear ($R^2 = 0.968$–0.995) and the slope is negative. A negative slope is indicative of a positive energy barrier. The activation energy is calculated from the slope of this graph, according to Eqs. (6) and (7). As shown in Table 4,

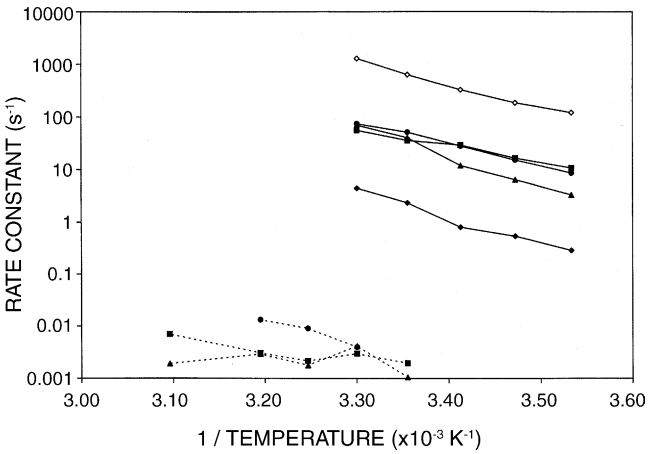

Fig. 5. Representative graph of the rate constant (k_{ms}) vs. inverse temperature used to calculate the activation energy. Mobile phase: methanol, 2085 psi, 0.08 cm/s (—); acetonitrile, 2185 psi, 0.08 cm/s (– – –). Symbols defined in Fig. 3. Other experimental details as given in the text.

Table 4
Activation energies and activation volumes for NPAHs in methanol mobile phase

Solute	$\Delta E_{\ddagger s}$ (kcal/mol)[a]	$\Delta E_{\ddagger m}$ (kcal/mol)[a]	$\Delta V_{\ddagger s}$ (mL/mol)[b]	$\Delta V_{\ddagger m}$ (mL/mol)[b]
1-Aminopyrene[c]	21 ± 1	16 ± 1	97 ± 20	99 ± 18
1-Azapyrene	24 ± 2	18 ± 2	47 ± 48	47 ± 44
4-Azapyrene	19 ± 1	14 ± 1	5 ± 6	6 ± 7
Benz[*a*]acridine	21 ± 3	14 ± 3	58 ± 36	51 ± 36
Dibenz[*a*,*j*]acridine	25 ± 1	16 ± 1	49 ± 15	38 ± 16

[a] Activation energies from stationary phase to transition state ($\Delta E_{\ddagger s}$) and from mobile phase to transition state ($\Delta E_{\ddagger m}$) calculated at $P = 2835$ psi.
[b] Activation volumes from stationary phase to transition state ($\Delta V_{\ddagger s}$) and from mobile phase to transition state ($\Delta V_{\ddagger m}$) calculated at $T = 288$ K, except as otherwise noted.
[c] Activation volumes calculated at $T = 283$ K.

the activation energies are positive for all solutes. The activation energy for the transfer from stationary phase to transition state ($\Delta E_{\ddagger s}$) is greater than that from mobile phase to transition state ($\Delta E_{\ddagger m}$). These data indicate that it is easier for the solutes to enter the stationary phase than to exit. The energy barriers $\Delta E_{\ddagger s}$ and $\Delta E_{\ddagger m}$ seem to be similar for all solutes and, indeed, there is no statistically significant difference. These values are comparable to those reported previously for the parent PAHs [28].

4.1.2.3. Activation volume. A representative graph of the natural logarithm of the rate constant versus pressure is shown in Fig. 6. The activation volume is calculated from the slope of this graph, according to Eqs. (8) and (9). As shown in Table 4, 1-aminopyrene has the largest activation volume while the other solutes are somewhat smaller. The values for the azapyrenes appear to be similar to those for the parent PAH, pyrene ($\Delta V_{\ddagger s} = 47 \pm 7$ mL/mol, $\Delta V_{\ddagger m} = 43 \pm 7$ mL/mol) [28]. However, the activation volumes for many of the NPAHs are statistically indistinguishable from zero, given the small effect of pressure and the correspondingly large standard deviation. Hence, no definitive conclusions can be drawn about the volumetric barrier for these solutes.

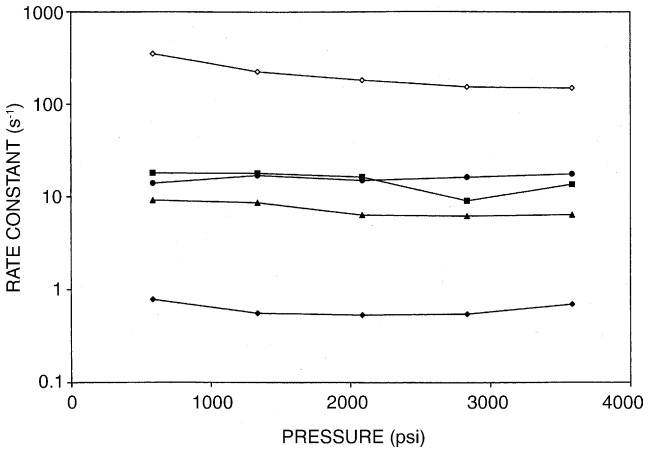

Fig. 6. Representative graph of the rate constant (k_{ms}) vs. pressure used to calculate the activation volume. Mobile phase: methanol, 283 K, 0.08 cm/s. Symbols defined in Fig. 3. Other experimental details as given in the text.

4.2. Acetonitrile mobile phase

In the previous study, the NPAHs showed evidence of a partition mechanism on the octadecylsilica stationary phase, similar to the parent PAHs, with some additional contributions that are attributable to adsorption. The methanol mobile phase used for this study is able to form hydrogen bonds with the NPAHs and thereby inhibit their ability to adsorb at silanol sites. At the same time, methanol can form hydrogen bonds with the silanol sites to displace or compete with the NPAHs. By these two mechanisms, the protic mobile phase can reduce interactions of the NPAHs with silanol sites. Therefore, it is beneficial to examine the effect of an aprotic solvent such as acetonitrile, which cannot undergo such hydrogen bonding interactions, on the combined partition–adsorption mechanism.

The effect of temperature on the thermodynamic and kinetic behavior of the NPAHs in the methanol mobile phase is significant (Tables 1 and 3), so that a large temperature range is also warranted in acetonitrile. A higher range of temperatures (293–333 K) is selected because of the greater retention and asymmetry of the zone profiles in acetonitrile (Fig. 2). In contrast, the effect of pressure on the thermodynamic and kinetic behavior is very small in the methanol mobile phase (Tables 1 and 3). Hence, the study in acetonitrile is conducted at a single average pressure of 2185 psi.

4.2.1. Thermodynamic behavior

4.2.1.1. Retention factor. Representative values of the retention factor for the NPAHs in acetonitrile mobile phase are summarized in Table 5. As shown, 1-aminopyrene is eluted first, followed by 4-azapyrene, benz[*a*]acridine, and dibenz[*a*,*j*]acridine. 1-Azapyrene is the most strongly

Table 5
Thermodynamic data for NPAHs in acetonitrile mobile phase

Solute	k[a]		ΔH_{sm} (kcal/mol)[a]
	303 K	313 K	
1-Aminopyrene	0.24	0.16	−6.3 ± 0.7
4-Azapyrene	4.55	2.74	−9.5 ± 1.1
Benz[*a*]acridine	4.48	4.15	−8.3 ± 2.1
Dibenz[*a*,*j*]acridine	6.43	5.49	−6.1 ± 2.1

[a] Retention factor (k) and change in molar enthalpy (ΔH_{sm}) calculated at $P = 2185$ psi.

retained solute and exhibited such severe asymmetry that it was excluded from the quantitative thermodynamic and kinetic studies.

When compared to the methanol mobile phase (Table 1), all solutes demonstrate an increase in retention factor in acetonitrile. Given that acetonitrile is less polar than methanol, the retention factor would be expected to decrease if the partition mechanism were predominant. Thus, the observed increase in retention factor suggests that the adsorption mechanism is contributing more greatly to retention in acetonitrile than in methanol. The increase is slight (4%) for 1-aminopyrene but very substantial (320–850%) for the aza-PAHs, which is consistent with the relative basicity of amine and aza groups, as discussed previously. In fact, the retention factors for the four-ring aza-PAHs are markedly larger than those for the parent PAHs [27,28], which suggests that the adsorption mechanism is predominant for these solutes in acetonitrile.

4.2.1.2. Molar enthalpy. A representative graph of the logarithm of the retention factor versus the inverse temperature is shown in Fig. 3. The data for the acetonitrile mobile phase are represented using dashed lines. It is evident that the retention data for 1-aminopyrene are nearly collinear in the acetonitrile and methanol mobile phases. This suggests that there is no significant difference in the retention mechanism for this solute. In contrast, the retention factors for the aza-PAHs are approximately an order-of-magnitude greater in acetonitrile than in methanol. Although the graph for each NPAH is linear, the square of the correlation coefficient is highly variable (R^2 = 0.724–0.986) because of the high degree of asymmetry and resulting uncertainty in the retention factor. It should be noted that the smallest correlation coefficients are exhibited by the aza-PAHs, which have the greatest asymmetry. The slope of the graph is positive, which is indicative of a negative change in molar enthalpy and suggests that the transfer from mobile to stationary phase is enthalpically favorable. The change in molar enthalpy is calculated from the slope of Fig. 3, according to Eq. (2).

As shown in Table 5, the changes in molar enthalpy are the least negative for 1-aminopyrene and dibenz[*a*,*j*]acridine and become progressively more negative for benz[*a*]acridine and 4-azapyrene. This order does not show the trends expected for the partition mechanism, i.e. more negative changes in molar enthalpy with increasing ring number and less condensed annelation structure. Rather, this order is consistent with the hydrogen bonding strength and steric effects at silanol groups, as discussed previously for the methanol mobile phase. The changes in molar enthalpy for the four-ring NPAHs are slightly more negative in acetonitrile than in methanol. 1-Aminopyrene, 4-azapyrene, and benz[*a*]acridine exhibit values that are 1.3, 3.7, and 1.7 kcal/mol more negative in acetonitrile than in methanol (Table 2). This change in molar enthalpy is consistent with the greater role of adsorption in the aprotic solvent, particularly for azapyrene. In contrast, the value for dibenz[*a*,*j*]acridine is 2.8 kcal/mol less negative in acetonitrile than in methanol. This suggests that the partition mechanism is still relatively important for this solute, such that the less polar mobile phase, acetonitrile, competes more effectively than methanol with the nonpolar stationary phase.

Although there are small and important differences, it is noteworthy that the changes in molar enthalpy are very similar in the acetonitrile and methanol mobile phases. Yet the retention factors for the aza-PAHs differ by nearly an order of magnitude in these mobile phases. From Fig. 3, it is evident that the difference lies in the intercept of the Van't Hoff plot. Again, according to Eq. (2), there are two possible origins of this difference. The entropy term may be substantially more negative in methanol because of the solvent release from both solute and silanol sites upon binding. A smaller entropy term in acetonitrile would lead to a larger value for the intercept. Alternatively, a change in the phase ratio may arise because of the greater number of free silanol groups in acetonitrile. In methanol, many of the silanol groups may be hydrogen bonded and not available for binding with the solute. The larger phase ratio in acetonitrile would also lead to a larger value for the intercept. As noted previously, it is difficult to discern which of these origins is prevailing by chromatographic methods alone.

4.2.2. Kinetic behavior

4.2.2.1. Rate constants. Representative values of the rate constants, calculated using Eqs. (4) and (5), are summarized in Table 6. 1-Aminopyrene undergoes much faster rates of transfer than 4-azapyrene, benz[*a*]acridine, and dibenz[*a*,*j*]acridine, which are two to three orders-of-magnitude slower. As in the methanol mobile phase, the rate-limiting step for 1-aminopyrene is the transfer from the acetonitrile mobile phase to the stationary phase. However,

Table 6
Kinetic data for NPAHs in acetonitrile mobile phase

Solute	k_{ms} (s^{-1})[a]		k_{sm} (s^{-1})[a]		$\Delta E_{‡s}$ (kcal/mol)[b]	$\Delta E_{‡m}$ (kcal/mol)[b]
	303 K	313 K	303 K	313 K		
1-Aminopyrene	3.47	3.67	8.2×10^{-1}	5.9×10^{-1}	~0	~0
4-Azapyrene	3.9×10^{-3}	1.3×10^{-2}	1.8×10^{-2}	3.6×10^{-2}	23 ± 5	13 ± 3
Benz[*a*]acridine	2.9×10^{-3}	3.0×10^{-3}	1.3×10^{-2}	1.3×10^{-2}	9 ± 3	~0
Dibenz[*a*,*j*]acridine	4.1×10^{-3}	2.9×10^{-3}	2.6×10^{-2}	1.6×10^{-2}	2 ± 6	~0

[a] Rate constants from stationary to mobile phase (k_{ms}) and from mobile to stationary phase (k_{sm}) calculated at P = 2185 psi.
[b] Activation energies from stationary phase to transition state ($\Delta E_{‡s}$) and from mobile phase to transition state ($\Delta E_{‡m}$) calculated at P = 2185 psi.

the aza-PAHs demonstrate the inverse trend, with the transfer from stationary to mobile phase serving as the rate-limiting step. When compared to the methanol mobile phase, the rate constants in acetonitrile are two to four orders-of-magnitude smaller. The differences in the rate constants result from the increased ability of the NPAHs to interact with the silica support. As noted previously, the aprotic solvent acetonitrile does not hydrogen bond to the solutes or to the silanol sites as does the protic solvent methanol. Hence, the rate constants from mobile to stationary phase and from stationary to mobile phase are substantially slower.

4.2.2.2. Activation energy. A representative graph of the logarithm of the rate constant versus the inverse temperature is shown in Fig. 5. The data for the acetonitrile mobile phase are represented using dashed lines. It should be noted that the data for 1-aminopyrene are not depicted in this graph. The zone profiles for 1-aminopyrene are nearly Gaussian and, as such, exhibit very small values of the asymmetric variance (τ^2). The small values of τ^2 result in calculated values for the rate constants (Eqs. (4) and (5)) that are highly variable as a function of temperature.

As shown in Fig. 5, the graph for each NPAHs is linear and the slope is negative. Unlike the graph for the methanol mobile phase, acetonitrile shows correlation coefficients for the linear regression that vary significantly ($R^2 = 0.038$–0.960). As such, the reported values should be used only to draw general conclusions. The activation energy is calculated from the slope of this graph, according to Eqs. (6) and (7). As shown in Table 6, the activation energies are positive for all of the NPAHs. The activation energy for the transfer from stationary phase to transition state ($\Delta E_{\ddagger s}$) is generally larger than that from mobile phase to transition state ($\Delta E_{\ddagger m}$). These data indicate that it is easier for the solutes to enter the stationary phase than to exit. In spite of the large standard deviations, the activation energy appears to be smallest for 1-aminopyrene, slightly greater for benz[*a*]acridine and dibenz[*a*,*j*]acridine, and greatest for 4-azapyrene.

5. Conclusions

In this study, the thermodynamic and kinetic behavior of NPAHs was examined in reversed-phase liquid chromatography. The parent PAHs are separated primarily by a partition mechanism with the octadecyl groups, but some minor interaction with the silanol groups can occur through the aromatic (π) system. In methanol mobile phase, the retention factors for the NPAHs are less than those for the parent PAHs. This is consistent with the partition mechanism, where retention decreases as the polarity of the solute increases. In addition, the trends of retention with ring number and annelation structure are consistent with the partition mechanism. However, the changes in molar enthalpy for the NPAHs indicate that adsorption at the silanol groups is more significant than for the parent PAHs. The observed changes reflect the relative basicity of the amine and aza groups, but also indicate that steric effects are important. The more condensed amino- and azapyrenes can diffuse more easily to the silanol groups than the more linear benz[*a*]acridine and dibenz[*a*,*j*]acridine. The importance of adsorption is also reflected in the kinetic rate constants, which are significantly smaller for the NPAHs than for the parent PAHs.

The trends in thermodynamic behavior in the protic solvent methanol become even more pronounced in the aprotic solvent acetonitrile. Methanol is able to hydrogen bond with the NPAH solutes as well as with the silanol groups, thereby reducing their mutual interactions. Acetonitrile is not able to shield interactions in this manner, hence the retention factors for the aza-PAHs are substantially greater than those in methanol. Moreover, the retention factors for the four-ring aza-PAHs are greater than those for the parent PAHs, which suggests that the adsorption mechanism is predominant for these solutes. The changes in molar enthalpy are slightly more negative for these solutes, but not sufficient to account for the large change in retention factor. Hence, we suggest that a significant change in entropy or the phase ratio is responsible for the thermodynamic behavior. The kinetic behavior also reflects the increased role of adsorption, with rate constants that are two to four orders-of-magnitude smaller than those in methanol. This thermodynamic and kinetic information provides a much clearer description of the retention mechanism of NPAHs in reversed-phase liquid chromatography. However, further studies with aqueous mobile phases and additives are desirable for more thorough characterization.

Acknowledgement

The authors gratefully acknowledge Dr. Lane C. Sander (National Institute of Standards and Technology) for synthesis of the polymeric octadecylsilica stationary phase.

References

[1] T. Vo-Dinh (Ed.), Chemical Analysis of Polycyclic Aromatic Hydrocarbons, Wiley, New York, 1988.
[2] M. Cooke, A.J. Dennis, G.L. Fisher (Eds.), Polynuclear Aromatic Hydrocarbons: Physical and Biological Chemistry, Battelle Press, Columbus, OH, 1982.
[3] R.F. Hertel, G. Rosner, J. Kielhorn (Eds.), Selected Non-Heterocyclic Polycyclic Aromatic Hydrocarbons, World Health Organization, Geneva, 1998.
[4] C.H. Ho, B.R. Clark, M.R. Guerin, B.D. Barkenbus, T.K. Rao, J.L. Epler, Mutat. Res. 85 (1981) 335.
[5] G.M. Seixas, B.M. Andon, P.G. Hollingshead, W.G. Thilly, Mutat. Res. 102 (1982) 201.
[6] A. Matsuoka, K. Shudo, Y. Saito, T. Sofuni, M. Ishidae, Mutat. Res. 102 (1982) 275.
[7] E.A.J. Bleeker, S. Wiegman, P. de Voogt, M. Kraak, H.A. Leslie, E. de Haas, W. Admiraal, Rev. Environ. Contam. Toxic. 173 (2001) 39.

[8] J.M. Schmitter, H. Colin, J.L. Excoffier, P. Arpino, G. Guiochon, Anal. Chem. 54 (1982) 769.
[9] S.C. Ruckmick, R.J. Hurtubise, J. Chromatogr. 321 (1985) 343.
[10] C. Borra, D. Wiesler, M. Novotny, Anal. Chem. 59 (1987) 339.
[11] N. Motohashi, K. Kamata, R. Meyer, Environ. Sci. Technol. 25 (1991) 342.
[12] J.M. Schmitter, I. Ignatiadis, G. Guiochon, J. Chromatogr. 248 (1982) 203.
[13] M.R. Guerin, C.H. Ho, T.K. Rao, B.R. Clark, J.L. Epler, Environ. Res. 23 (1980) 42.
[14] S.G. Wakeham, Environ. Sci. Technol. 13 (1979) 1118.
[15] H.Y. Chen, M.R. Preston, Environ. Sci. Technol. 32 (1998) 577.
[16] M. Wilhelm, G. Matuschek, A. Kettrup, J. Chromatogr. A 878 (2000) 171.
[17] K. Kamata, N. Motohashi, J. Chromatogr. 319 (1985) 331.
[18] K. Kamata, N. Motohashi, R. Meyer, Y. Yamamoto, J. Chromatogr. 596 (1992) 233.
[19] K. Kamata, N. Motohashi, J. Chromatogr. 396 (1987) 437.
[20] M. Ashraf-Khorassani, L.T. Taylor, J. Chromatogr. Sci. 26 (1988) 331.
[21] H. Colin, J.M. Schmitter, G. Guiochon, Anal. Chem. 53 (1981) 625.
[22] A.M. Siouffi, M. Righezza, G. Guiochon, J. Chromatogr. 368 (1986) 189.
[23] T.R. Steinheimer, M.G. Ondrus, Anal. Chem. 58 (1986) 1839.
[24] J.W. Haas, W.F. Joyce, Y.J. Shyu, P.C. Uden, J. Chromatogr. 457 (1988) 215.
[25] K. Kamata, N. Motohashi, J. Chromatogr. 498 (1990) 129.
[26] H. Carlsson, C. Östman, J. Chromatogr. A 715 (1995) 31.
[27] S.B. Howerton, V.L. McGuffin, Anal. Chem. 75 (2003) 3539.
[28] S.B. Howerton, V.L. McGuffin, J. Chromatogr. A 1030 (2004) 3.
[29] S.A. Wise, W.J. Bonnett, F.R. Guenther, W.E. May, J. Chromatogr. Sci. 19 (1981) 457.
[30] V.L. McGuffin, C. Lee, J. Chromatogr. A 987 (2003) 3.
[31] K.J. Laidler, Chemical Kinetics, third ed., Harper & Row, New York, 1987.
[32] J.I. Steinfeld, J.S. Francisco, W.L. Hase, Chemical Kinetics and Dynamics, second ed., Prentice Hall, Upper Saddle River, NJ, 1999.
[33] V.L. McGuffin, S.H. Chen, J. Chromatogr. A 762 (1997) 35.
[34] J.C. Gluckman, A. Hirose, V.L. McGuffin, M. Novotny, Chromatographia 17 (1983) 303.
[35] S.B. Howerton, C. Lee, V.L. McGuffin, Anal. Chim. Acta 478 (2003) 99.
[36] H.C. Thomas, J. Am. Chem. Soc. 66 (1944) 1664.
[37] J.L. Wade, A.F. Bergold, P.W. Carr, Anal. Chem. 59 (1987) 1286.
[38] J.H. Hildebrand, R.L. Scott, The Solubility of Nonelectrolytes, third ed., Reinhold, New York, 1950.
[39] M.W. Ducey, C.J. Orendorff, J.E. Pemberton, L.C. Sander, Anal. Chem. 74 (2002) 5576.
[40] M.W. Ducey, C.J. Orendorff, J.E. Pemberton, L.C. Sander, Anal. Chem. 74 (2002) 5585.
[41] A. Nahum, C. Horvath, J. Chromatogr. 203 (1981) 53.
[42] R.A. Matzner, R.C. Bales, J.E. Pemberton, Appl. Spectrosc. 48 (1994) 1043.
[43] S.C. Ringwald, J.E. Pemberton, Environ. Sci. Technol. 34 (2000) 259.
[44] D.R. Lide, Handbook of Chemistry and Physics, 71st ed., CRC Press, Boca Raton, FL, 1990.
[45] B.N. Woodrow, J.G. Dorsey, Environ. Sci. Technol. 31 (1997) 2812.
[46] R. Matzner, R.C. Bales, Chemosphere 29 (1994) 1755.
[47] R. Matzner, R.C. Bales, J. Colloid Interface Sci. 168 (1994) 61.